Adsorption Kinetics of Nonanol at the Air−Water Interface: Considering Molecular Interaction or Aggregation within Surface Layer

ARTICLE *in* LANGMUIR · APRIL 2002

Impact Factor: 4.46 · DOI: 10.1021/la011418t · Source: OAI

5 AUTHORS, INCLUDING:

Hwai-Shen Liu
National Taiwan University
83 PUBLICATIONS **1,151** CITATIONS

Adsorption Kinetics of Nonanol at the Air−Water Interface: Considering Molecular Interaction or Aggregation within Surface Layer

Ya-Chi Lee,[†] Yu-Bing Liou,[‡] Reinhard Miller,[§] Hwai-Shen Liu,[†] and Shi-Yow Lin*,[‡]

Department of Chemical Engineering, National Taiwan University, 1 Roosevelt Road, Sec. 4, Taipei, 106 Taiwan, Chemical Engineering Department, National Taiwan University of Science and Technology, 43, Keelung Road, Sec. 4, Taipei, 106 Taiwan, and Max-Planck-Institut für Kolloid- und Grenzflächenforschung, Max-Planck-Campus, Haus 2, Am Mühlenberg 2, D-14476 Golm/Potsdam, Germany

Received September 11, 2001. In Final Form: January 2, 2002

The adsorption kinetics of 1-nonanol at the air−water interface was investigated. A video-enhanced pendant bubble tensiometer was applied for the measurement of equilibrium and dynamic surface tension. Two sets of equilibrium data $\gamma(C)$ and $\gamma(\Gamma)$ (equation of state) and two sets of surface tension relaxations $\gamma(t)$, for the adsorption of 1-nonanol onto a freshly created interface and for the desorption out of a suddenly compressed interface, were measured. The data are analyzed by either considering the molecular interaction between the adsorbed molecules or assuming that surfactant molecules form two-dimensional aggregates. Both models fit the equilibrium $\gamma(C)$ and dynamic $\gamma(t)$ data very well, and similar results are obtained: (i) the adsorption of 1-nonanol is cooperative (from the $\gamma(C)$ data) and (ii) the adsorption onto a fresh interface is diffusion controlled (from the $\gamma(t)$ data).

1. Introduction

The Langmuir adsorption isotherm assumes that there exists no molecular interaction in system, neither in bulk nor at fluid interface. Lin et al.[1−3] had reported that the adsorption behavior of 1-decanol deviates significantly from the Langmuir model due to a strong interaction between the adsorbed molecules at the air−water interface. A cusp, or near cusp behavior in the $\gamma-\ln(C)$ curve, and a slow initial rate of surface tension decrease are evidences of the strong attractive energies between surface-adsorbed 1-decanol molecules with increasing surface coverage. MacLeod and Radke[4] and Johnson and Stebe[5] also reported a strong molecular interaction among the adsorbed 1-decanol molecules.

Fainerman and Miller[6] and Aksenenko et al.[7] confirmed the deviation of 1-decanol from the Langmuir-type behavior by assuming a 2D aggregation within the surface layer. The aggregation model with a mean aggregation number of 2.5 describes satisfactorily the experimental $\gamma(C)$ and $\gamma(t)$ data. A reorientation model, which considers the change in the partial molar area with increasing surface pressure due to molecular orientation, has also been proposed to describe the nonideal adsorption behavior of fatty alcohols at liquid interfaces.[8−10]

The adsorption kinetics for the long chain alcohols (octanol, nonanol, and decanol) have been intensely studied for last two decades. Many articles have reported that the adsorption kinetics of octanol and decanol are diffusion controlled.[4,5,11−21] Fainerman and Lylyk[14] applied the maximum bubble pressure method for the measurement of dynamic surface tension of nonanol. A comparison on the adsorption kinetics of different alcohols has been detailed in ref 22.

The aim of this work is to investigate the adsorption mechanism of 1-nonanol. A video-enhanced pendant bubble tensiometer was employed for the measurement of surface tension relaxation. Different models (the Frumkin, generalized Frumkin, and aggregation) are applied to describe the equilibrium and dynamic data of surface tension at 25 °C. The equilibrium data consist of the equilibrium surface tension (γ vs ln$C$) and the equation

* To whom correspondence should be addressed. Tel: 886-2-2737-6648. Fax: 886-2-2737-6644. E-mail: ling@ch.ntust.edu.tw.
[†] National Taiwan University.
[‡] National Taiwan University of Science and Technology.
[§] Max-Planck-Institut für Kolloid- und Grenzflächenforschung.

(1) Lin, S. Y.; McKeigue, K.; Maldarelli, C. *Langmuir* **1991**, *7*, 1055.
(2) Lin, S. Y.; Lu, T. L.; Hwang, W. B. *Langmuir* **1995**, *11*, 555.
(3) Lin, S. Y.; Hwang, W. B.; Lu, T. L. *Colloids Surf., A* **1996**, *114*, 143.
(4) MacLeod, C. A.; Radke, C. J. *J. Colloid Interface Sci.* **1993**, *160*, 435.
(5) Johnson, D. O.; Stebe, K. J. *J. Colloid Interface Sci.* **1996**, *182*, 526.
(6) Fainerman, V. B.; Miller, R. *Langmuir* **1996**, *12*, 6011.
(7) Aksenenko, E. V.; Fainerman, V. B.; Miller, R. *J. Phys. Chem.* **1998**, *102*, 6025.
(8) Fainerman, V. B.; Miller, R.; Wüstneck, R.; Makievski, A. V. *J. Phys. Chem.* **1996**, *100*, 7669.
(9) Miller, R.; Aksenenko, E. V.; Liggieri, L.; Ravera, F.; Ferrari, M.; Fainerman, V. B. *Langmuir* **1999**, *15*, 1328.
(10) Fainerman, V. B.; Miller, R.; Aksenenko, E. V.; Makievski, A. V.; Krägel, J.; Loglio, G.; Liggieri, L. *Adv. Colloid Interface Sci.* **2000**, *86*, 83.
(11) Defay R.; Hommelen, J. R. *J. Colloid Sci.* **1958**, *13*, 553.
(12) Defay R.; Hommelen, J. R. *J. Colloid Sci.* **1959**, *14*, 411.
(13) Rillaerts, E.; Joos, P. *J. Phys. Chem.* **1982**, *86*, 3471.
(14) Fainerman, V. B.; Lylyk, S. V. *Kolloidn. Zh.* **1982**, *44*, 538.
(15) Fainerman, V. B.; Lylyk, S. V. *Kolloidn. Zh.* **1983**, *45*, 500.
(16) Bleys, G.; Joos, P. *J. Phys. Chem.* **1985**, *89*, 1027.
(17) Chang, C. H.; Franses, E. I. *Colloids Surf.* **1992**, *69*, 189.
(18) Uffelen, M. V.; Joos, P. *J. Colloid Interface Sci.* **1993**, *158*, 452.
(19) Chang, C. H.; Franses, E. I. *Chem. Eng. Sci.* **1994**, *49*, 313.
(20) Defay R.; Hommelen, J. R. *J. Colloid Sci.* **1959**, *14*, 401.
(21) Joos, P.; Uffelen, M. V. *J. Colloid Interface Sci.* **1993**, *155*, 271.
(22) Stebe, K.; Lin, S. Y. Dynamic Surface Tension and Surfactant Mass Transfer Kinetics: Measurement Techniques and Analysis. In *Handbook of Surfaces and Interfaces of Materials*; Nalwa, H. S., Ed.; Academic Press: London 2001; Vol. 2

10.1021/la011418t CCC: $22.00
Published on Web 02/22/2002

of state (γ vs Γ/Γ_{ref}). The dynamic surface tension in two processes are measured: the adsorption onto a freshly created air−water interface in a quiescent solution and the desorption out of a covered surface due to a sudden compression on an air bubble. A comparison of the results obtained from different models is given.

2. Experimental Measurements

Materials. Nonionic surfactant 1-nonanol ($C_9H_{19}OH$, >99% purity) purchased from Aldrich was used without modification. Water was purified via a Barnstead NANOpure water purification system.

Pendant Bubble. A video-enhanced pendant bubble tensiometer[23−26] was employed for the measurement of equilibrium surface tension $\gamma(C)$, equation of state $\gamma(\Gamma)$, and dynamic surface tension $\gamma(t)$ of aqueous nonanol solutions. The apparatus and the edge detection routine have been described in detail in previous studies.[23] The temperature variation of aqueous solution is less than ±0.05 K.[26] A 17-gauge stainless steel inverted needle (1.07 mm i.d.; 1.47 mm o.d.) was used for the bubble generation.

Adsorption. A pendant bubble of air with a diameter of ca. 2 mm was formed in a nonanol solution, which was put in a quartz cell. Digital images of the bubble were taken sequentially and then processed to determine the surface area and surface tension. The time required to create an air bubble in this work is about 2.2 s, therefore the time of 1.1 s (half of the formation time) is added to evaluate a more accurate surface age.

The measurement was performed for 15 different bulk concentrations (1×10^{-8} to 3.5×10^{-7} mol/cm^3), and each sample was repeated 3−5 times. The bubbles were measured up to around 1/3−3 h, depending on the surfactant concentration.

Surface Expansion. When the adsorption reached the equilibrium state, the air−water surface was expanded and sequential digital images of the bubble were taken. At each concentration (0.85, and 1.2×10^{-7} mol/cm^3), it was repeated 10 times with expansion rate $dA/dt = 2.9-16$ mm^2/s. From the dynamic data of surface area $A(t)$, dA/dt, and $\gamma(t)$, $\gamma-t$ and $\gamma-A$ dependencies were obtained. A unique dependence between γ and A/A_{ref} (relative surface area) for those runs with large dA/dt was obtained.[27,28] This implies that there is nearly no surfactant molecule adsorbing onto the expanding surface during the expansion process at large expansion rate. A unique curve relating γ and relative surface concentration (Γ/Γ_{ref}), i.e., the equation of state, is then obtained and utilized on the determination of adsorption isotherm and model parameters.

Desorption. When the adsorption of 1-nonanol had reached the equilibrium state, a small part of air inside the bubble was allowed to leave and the bubble surface area decreased abruptly around 10−17%.[29,30] The images were recorded on a recorder as well as taken sequentially onto the computer during the shrinkage of bubble. The images were then processed to obtain the surface area and surface tension.

Surface Tension. The edge coordinates of pendant bubble are best-fitted with the theoretical shape generated from the classical Laplace equation. The accuracy and reproducibility of the γ measurements are ca. 0.1 mN/m.[25,26]

3. Theoretical Framework

The mass transport of 1-nonanol molecules between the air−water interface and the bulk phase of a quiescent surfactant solution are modeled. Two approaches are considered: (i) models utilize the Langmuir formalism with the consideration of molecular interaction between the adsorbed 1-nonanol molecules and (ii) models assume a 2D aggregation within the surface layer. Nonanol is assumed not to dissolve into the gas phase of the bubble, and the convection effect is negligible.

Case I. Frumkin and Generalized Frumkin Models. In this approach, the mass transport in bulk is considered to be a 1D diffusion onto or out of a spherical surface. Bulk diffusion is considered to be spherical symmetric. A modified Ward and Tordai equation results from refs 22 and 23

$$\Gamma(t) = \Gamma_b + (D/b)[C_0 t - \int_0^t C_s(\tau)\, d\tau] + 2(D/\pi)^{1/2}[C_0 t^{1/2} - \int_0^{\sqrt{t}} C_s(t-\tau)\, d\tau^{1/2}] \quad (1)$$

where D denotes the diffusivity, $C_s(t)$ is the subsurface concentration, $\Gamma(t)$ is the surface concentration, Γ_b is the initial surface concentration and is equal to zero for a fresh interface, b is the bubble radius, and C_0 is the bulk concentration far from the bubble surface.

The adsorption equation used here utilizes the Langmuir formalism and assumes that the rate of mass transport across the interface depends on the activation energies of the adsorption and desorption processes.[31] The activation energies are Γ dependent with a power law ($E_a = E_a^0 + \nu_a\Gamma^n$ and $E_d = E_d^0 + \nu_d\Gamma^n$ with constants E_a^0, E_d^0, ν_a, and ν_d)

$$d\Gamma/dt = \beta \exp(-E_a/RT) C_s(\Gamma_\infty - \Gamma) - \alpha \exp(-E_d/RT)\Gamma \quad (2)$$

$$\frac{\Gamma}{\Gamma_\infty} = x = \frac{C}{C + a \exp(Kx^n)} \quad (3)$$

where β and α are the pre-exponential factors, C is the bulk concentration of surfactant solution, T is the temperature, R is the gas constant, Γ_∞ is the maximum surface concentration, K [$= (\nu_a - \nu_d)\Gamma_\infty^n/RT$], and a and n are the parameters. Parameter K takes into account the molecular interaction between the adsorbed surfactants, and a indicates the surfactant activity.

Equation 3 becomes the Frumkin isotherm,[32,33] which assumes a linear dependence between E_a vs Γ and E_d vs Γ. The Langmuir adsorption isotherm results when E_a and E_d are independent of Γ. The presence of cohesive intermolecular forces, which lower the desorption rate at increasing Γ, is described by $K < 0$.[34,35] A positive K indicates an anti-cooperative adsorption, indicating that the adsorption becomes more difficult at increasing Γ.

On the theoretical simulation, the concentration of 1-nonanol on bubble surface is assumed to be equal to a constant initial surface concentration Γ_b. $\Gamma_b = 0$ for a clean adsorption process, in which the bubble was created suddenly. For the re-equilibration process due to a sudden surface compression, Γ_b was assumed to be equal to the surface coverage corresponding to the point with the lowest surface tension.

(23) Lin, S. Y.; McKeigue, K.; Maldarelli, C. *AIChE J.* **1990**, *36*, 1785.
(24) Lin, S. Y.; Hwang, H. F. *Langmuir* **1994**, *10*, 4703.
(25) Lin, S. Y.; Chen, L. J.; Xyu, J. W.; Wang, W. J. *Langmuir* **1995**, *11*, 4159.
(26) Lin, S. Y.; Wang, W. J.; Lin, L. W.; Chen, L. J. *Colloids Surf., A* **1996**, *114*, 31.
(27) Hsu, C. T.; Shao, M. J.; Lin, S. Y. *Langmuir* **2000**, *16*, 3187.
(28) Lin, S. Y.; Lee, Y. C.; Shao, M. J.; Hsu, C. T. *J. Colloid Interface Sci.* **2001**, *244*, 372.
(29) Tsay, R. Y.; Lin, S. Y.; Lin, L. W.; Chen, S. I. *Langmuir* **1997**, *13*, 3191.
(30) Hsu, C. T.; Shao, M. J.; Lee, Y. C.; Lin, S. Y. *Langmuir* **2000**, *16*, 4846.
(31) Lin, S. Y.; Wang, W. J.; Hsu, C. T. *Langmuir* **1997**, *13*, 6211.
(32) Frumkin, A. *Z. Phys. Chem.* (*Leipzig*) **1925**, *116*, 466.
(33) Lin, S. Y.; McKeigue, K.; Maldarelli, C. *Langmuir* **1994**, *10*, 3442.
(34) Borwankar R. P.; Wasan D. T. *Chem. Eng. Sci.* **1983**, *38*, 1637.
(35) Ferri, J. K.; Stebe, K. J. *J. Colloid Interface Sci.* **1999**, *209*, 1.

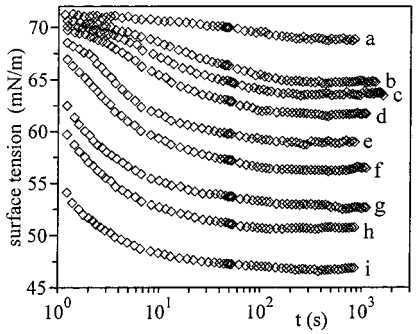

Figure 1. Representative dynamic surface tensions for adsorption of 1-nonanol onto a clean air−water interface for C_0 = (a) 0.50, (b) 0.75, (c) 0.85, (d) 1.0, (e) 1.2, (f) 1.5, (g) 2.0, (h) 2.5, and (i) 3.5 (10^{-7} mol/cm^3).

For an ideal solution, the Gibbs adsorption equation $d\gamma = -\Gamma RT\, d\ln C$ and the equilibrium isotherm (eq 3) allow for the calculation of the surface tension

$$\gamma - \gamma_0 = \Gamma_\infty RT[\ln(1 - x) - Knx^{n+1}/2] \qquad (4)$$

where γ_0 is the surface tension of pure water. By fitting the data of $\gamma(C)$ and of $\gamma(\Gamma)$, the equilibrium constants (K, a, n, and the maximum coverage Γ_∞) result.

Case II. Aggregation Model. Since the only available software package[36] is restricted to planar interfaces, only the case of 1D diffusion and adsorption onto a planar surface from a uniform bulk phase is considered. The Ward and Tordai equation and the adsorption isotherms have been described in detail in previous studies.[6−10,36] The result of the theoretical model is the following integral equation

$$\Gamma(t) = 2(D/\pi)^{1/2}\,[C_0 t^{1/2} - \int_0^{\sqrt{t}} C_s(t - \tau)\, d\tau^{1/2}] \qquad (5)$$

Together with the respective adsorption isotherm we obtain a complete set of equations to describe the adsorption process.[36]

For monodisperse aggregates formed within the adsorption surface layer, the following isotherm and equation of state are obtained from ref 8

$$C/a = \Gamma_1\omega/\{1 - \Gamma_1\omega[1 + (\Gamma_1/\Gamma_c)^{n-1}]\}^{\omega_1/\omega} \qquad (6)$$

$$-\Pi\omega/RT = \ln(1 - \Gamma\omega) \qquad (7)$$

where $\omega/\omega_1 = [1 + n(\Gamma_1/\Gamma_c)^{n-1}]/[1 + (\Gamma_1/\Gamma_c)^{n-1}]$, ω is the mean partial molar area of monomers and aggregates, Γ_1 and Γ_n are the values of adsorption of monomers and aggregates, $\Gamma(= \Gamma_1 + \Gamma_n)$ is the total adsorption, and Π is surface pressure ($= \gamma_0 - \gamma$). The model parameters are ω_1 (partial molar area of monomers), Γ_c (critical adsorption of aggregation), n (n-mers, aggregates within the surface layer), and a (adsorption equilibrium constant).

4. Experimental Results

Adsorption. Dynamic surface tension for the adsorption of 1-nonanol onto a clean air−water interface was measured up to 1/3−3 h from the moment (referenced as $t = 0$) at which one-half of the bubble volume is generated during the bubble formation. Shown in Figure 1 are representative dynamic surface tension profiles (for one selected bubble at each bulk concentration) of solutions

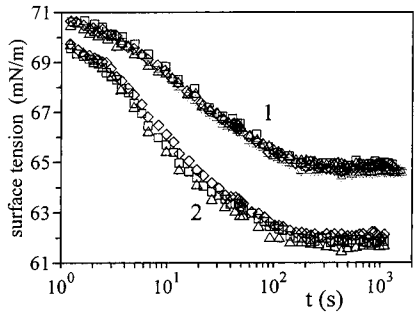

Figure 2. Experimental dynamic surface tensions for the adsorption of 1-nonanol onto a clean air−water interface for C_0 = (1) 0.75 and (2) 1.0 (10^{-7} mol/cm^3). Each symbol represents a separate bubble.

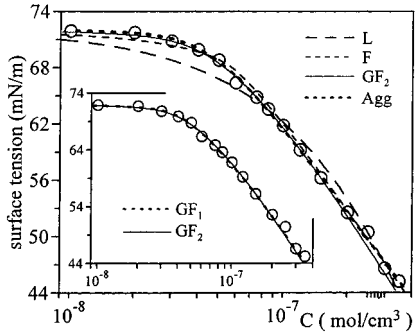

Figure 3. Equilibrium surface tension for air−nonanol aqueous solution and the theoretical predictions of the Langmuir (L), Frumkin (F), generalized Frumkin (GF_1 and GF_2), and aggregation (Agg) isotherms. Profiles of L, F, and GF_1 are from best-fitting only the $\gamma(C)$ data, GF_2 from best-fitting both $\gamma(C)$ and $\gamma(\Gamma)$ data, and Agg from best-fitting $\gamma(C)$ and dynamic $\gamma(t)$ data.

at nine different concentrations, $C = 0.50$, 0.75, 0.85, 1.0, 1.2, 1.5, 2.0, 2.5, and 3.0 (10^{-7} mol/cm^3). The reproducibility of these profiles is demonstrated in Figure 2. The equilibrium surface tensions were extracted from the long-time asymptotes in Figures 1 and 2 and are plotted in Figure 3.

Surface Expansion. The pendant bubble tensiometer worked as a Langmuir trough to find out the $\pi-A$ and $\gamma-\Gamma$ dependencies for soluble 1-nonanol. Figure 4 (parts a and b) shows a set of representative relaxation profiles of γ and surface area A of bubble during surface expansion for $C = 0.85 \times 10^{-7}$ mol/cm^3. The expansion rate of surface is obtained from the slope of the A vs t profile shown in Figure 4b. The data in Figures 4a and 4b are re-plotted in Figure 4c to show the γ vs A/A_{ref} relationship.

During the expansion, the γ goes up as A increases, indicating a depletion of surface concentration. Figure 4c shows the dependence of γ vs $A/A_{\gamma=67}$, in which the surface area at $\gamma = 67$ mN/m is picked as the reference point. A nearly unique $\gamma-A/A_{\gamma=67}$ profile results when $dA/dt > 14$ mm^2/s. For these runs, it takes less than or about 1 s for the surface area to expand from ca. 21 to 33 mm^2. While at a lower expansion rate (e.g., the squares, $dA/dt = 8.0$ mm^2/s), a deviation from the unique profile is observed. This indicates that there is a significant amount of surfactant molecules that adsorbs onto the surface during the surface-expansion process if dA/dt is low. For $C = 1.2 \times 10^{-7}$ mol/cm^3, 10 runs with different dA/dt ranging between 6.0 and 16.1 mm^2/s are performed, but no unique $\gamma-A/A_{ref}$ profile is observed. In other words, at this concentration, dA/dt must be larger than 16.1 mm^2/s for the process to have a negligible adsorption of nonanol during the surface-expansion process. The limiting dA/dt

(36) Aksenenko, E. V. Surfactants−Chemistry, Interfacial Properties, Applications. In *Studies in Interface Science*; Fainerman, V. B., Möbius, D., Miller, R., Eds.; Elsevier: 2001; Vol. 13, Chapter 7.

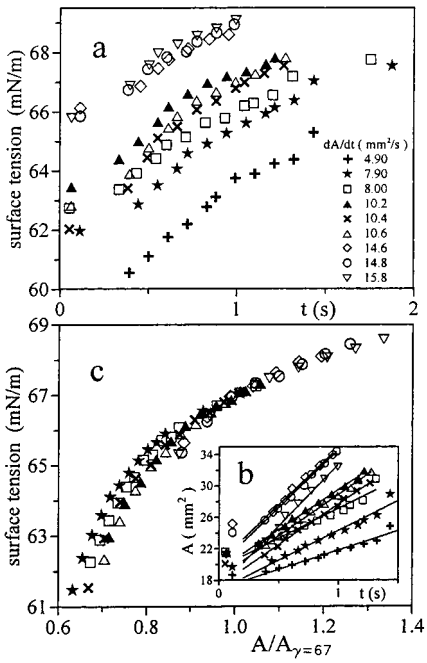

Figure 4. Experimental data of (a) surface tension (γ) vs time (t), (b) surface area (A) vs t for the expansion experiment, and (c) the influence of dA/dt on the dependence of between γ vs A/A_{ref}. $C_0 = 8.5 \times 10^{-8}$ mol/cm^3. Each symbol represents a separate run with different expansion rate (dA/dt).

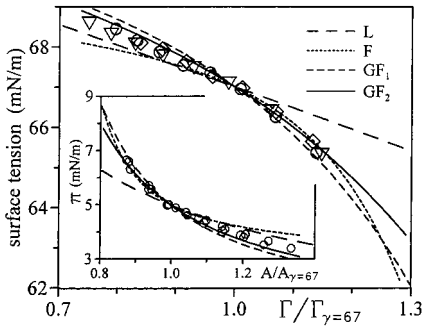

Figure 5. Comparison between the experimental data and the model predictions from the Langmuir (L), Frumkin (F), and generalized Frumkin (GF_1 and GF_2) isotherms for surface tension vs relative surface concentration and surface pressure (π) vs relative surface area.

for obtaining a unique $\gamma-A/A_{ref}$ profile depends on bulk concentration and the working surface area. For a higher concentration and/or a wider working range of surface area, a higher limiting expansion rate is needed.

The unique profile in Figure 4c is recalculated to obtain the $\gamma-\Gamma/\Gamma_{\gamma=67}$ and $\pi-A/A_{\gamma=67}$ relationships (Figure 5). If the adsorption of surfactant molecules during the expansion process is negligible, this unique profile represents the equilibrium surface property (equation of state) of 1-nonanol and can be used for the determination of the adsorption isotherm and model parameters.

Desorption. The re-equilibration process due to the desorption of 1-nonanol out of a suddenly compressed air−water surface was measured. The surface had reached the equilibrium state (with an equilibrium surface tension γ_e) before it was perturbed. Images were recorded up to 1000 s. The experiments were done five times at $C = 7.5 \times 10^{-7}$ mol/cm^3. In each run, the surface area was compressed with a different percentage (10−17%). All runs showed a similar behavior: surface tension decreased abruptly from the equilibrium value to a lower one and then increased smoothly up to its equilibrium value after the abrupt falling.

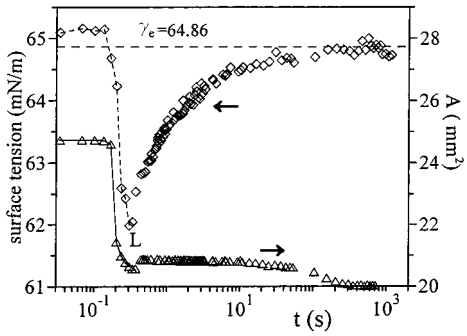

Figure 6. Representative dynamic surface tension and surface area of the pendant bubble for the re-equilibration process due to a sudden surface compression for 1-nonanol aqueous solutions. $C_0 = 7.5 \times 10^{-8}$ mol/cm^3.

A set of representative relaxation profiles of surface tension (the diamonds) and surface area (the triangles) of the bubble are shown in Figure 6. The surface tension decreased from the equilibrium value to a lower value (point L), corresponding to a higher surface coverage than the equilibrium one, in 0.167 s. The surface tension then increased and went back to the equilibrium tension in about 100 s. The bubble surface area decreased by 17% in 0.2 s and then maintained a nearly constant value.

Surface Coverage. Since the working concentrations of nonanol in this work are dilute, one can assume that the solutions are ideal and apply the Gibbs adsorption equation $d\gamma = -\Gamma RT\ d\ln C$ to estimate the surface concentrations (Γ) at different bulk concentrations. The Γ at bulk concentrations near the solubility of nonanol is evaluated from the equilibrium surface tension data and is equal to 5.4×10^{-10} mol/cm^2. This number is close to that obtained from the neutron reflection study by Li et al.[37] for butanol (6.2×10^{-10} mol/cm^2) and hexanol (5.9×10^{-10} mol/cm^2).

5. Modeling

Case I. Frumkin and Generalized Frumkin Models. In this case, two sets of equilibrium data are coupled to determine the adsorption isotherm and the model constants.

Model Determination. Usually, the equilibrium $\gamma(C)$ data were applied for determining the adsorption isotherm and model constants Γ_∞, a, K, and n. Equation 3 becomes the Langmuir adsorption isotherm when $K = 0$. As $n = 1$, eq 3 is the Frumkin isotherm. The Langmuir isotherm poorly predicts the $\gamma(C)$ data of 1-nonanol (Figure 3). The Frumkin isotherm has a better prediction than the Langmuir model but predicts a slightly lower γ at $C < 4.0 \times 10^{-8}$ mol/cm^3. This underestimation on γ makes a poor prediction on dynamic $\gamma(t)$ for $\gamma > 68$ mN/m as shown in Figure 7 (the dotted curve for 1×10^{-7} mol/cm^3). The generalized Frumkin isotherm fits the $\gamma(C)$ data nearly exactly (dashed curve GF_1). The model constants are listed in Table 1.

It was recently proposed[38] that if an incorrect adsorption isotherm is applied to fit the equilibrium $\gamma(C)$ and dynamic $\gamma(t)$ data, the model may describe the $\gamma(C)$ and $\gamma(t)$ profiles satisfactorily. However, a significant deviation may result

(37) Li, Z. X.; Lu, J. R.; Thomas, R. K.; Rennie, A. R.; Penfold, J. *J. Chem. Soc., Faraday Trans.* **1996**, *92*, 565.
(38) Hsu, C. T.; Chang, C. H.; Lin, S. Y. *Langmuir* **1997**, *13*, 6204; **1999**, *15*, 1952; **2000**, *16*, 1211.

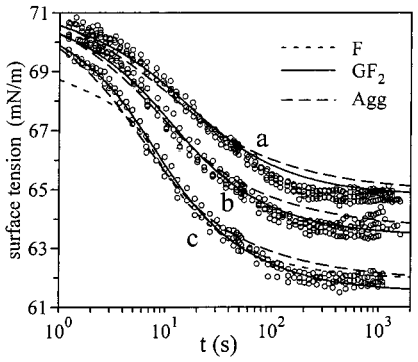

Figure 7. Comparison between dynamic $\gamma(t)$ data and the model predictions of diffusion-control for the Frumkin (F), generalized Frumkin (GF_2), and aggregation (Agg) models for C_0 = (a) 0.75, (b) 0.85, and (c) 1.0 (10^{-7} mol/cm^3).

Table 1. Model Constants of Optimal Fit for 1-nonanol Aqueous Solution

model[a]	$\Gamma_\infty \times 10^{10}$ (mol/cm^2)	a (mol/cm^3)	K	n	K/K_c[b]
L[c]	19.0	4.310×10^{-7}			
F[c]	5.91	3.137×10^{-7}	−3.410	1	0.85
GF_1[c]	6.377	3.002×10^{-6}	−4.972	0.291	0.73
GF_2[d]	6.789	3.774×10^{-6}	−5.00	0.253	0.67

[a] L = Langmuir, F = Frumkin, and GF = generalized Frumkin isotherm. [b] K_c = critical K value = $-(1 + 1/n)^{1+n}$. [c] From the best-fit with $\gamma(C)$. [d] From the best-fit with $\gamma(C)$ and $\gamma(\Gamma)$.

on diffusivity. For cooperative surfactants, a smaller diffusivity (D) is observed, and a larger D results for anti-cooperative surfactants.

To improve the theoretical modeling, the measured γ-(Γ/Γ_{ref}) curve (Figure 5) was utilized, coupled with the $\gamma(C)$ data, for the determination of adsorption isotherm and model constants. The solid curves (GF_2) in Figures 3 and 5 show the prediction from the generalized Frumkin isotherm. The model constants of GF_2 are also listed in Table 1. The fit on $\gamma(C)$ for GF_2 is as good as that on GF_1 (Figure 3). However, GF_2 predicts the $\gamma(\Gamma/\Gamma_{ref})$ data better than GF_1 (Figure 5).

The GF_2 model predicts the $\gamma(C)$ and $\gamma(\Gamma)$ profiles much better than F and L. The more exact agreement of GF_2 on $\gamma(\Gamma)$ data indicates that the molecular interactions between the adsorbed 1-nonanol molecules are significant and the assumption of a linear dependence between the activation energy and the surface concentration is not good enough for 1-nonanol. A power law ($E = E^0 + \nu\Gamma^n$) with n of around a quarter better describes the equilibrium data of 1-nonanol. Therefore, the GF_2 isotherm is picked for modeling the dynamic $\gamma(t)$ data below.

Both the Frumkin and generalized Frumkin models predict a negative K value from the equilibrium data of $\gamma(C)$ and γ (Γ/Γ_{ref}). This negative K indicates that the adsorption is a cooperative process, and the desorption becomes more difficult as the surface gets covered with more 1-nonanol molecules.

Diffusion-Control Adsorption. If the adsorption of 1-nonanol onto a freshly created air−water interface was assumed to be diffusion controlled, the data in Figure 1 can be used to determine the diffusivity (D) of 1-nonanol molecules. The set of model constants (GF_2 in Table 1) used here is what best-fits both sets of equilibrium data $\gamma(C)$ and $\gamma(\Gamma/\Gamma_{ref})$. As shown in Figure 7, the agreement between the dynamic data and the theoretical relaxation profiles is pretty good. Figure 8 shows the D (the triangles) from the best fit. A nearly constant D results except at C = 5.0×10^{-8} mol/cm^3 (the filled triangle). An average D of 6.3×10^{-6} cm^2/s resulted from the data of open triangles.

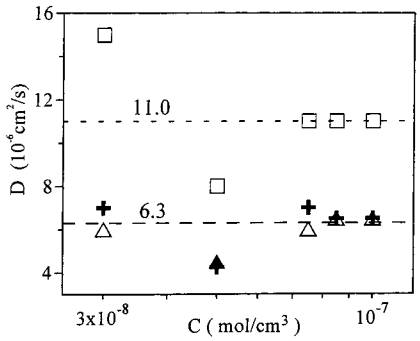

Figure 8. Diffusivities from the best-fit between $\gamma(t)$ data and model predictions from the generalized Frumkin (+, GF_1 and △, GF_2) and aggregation (□) models as a function of bulk concentration.

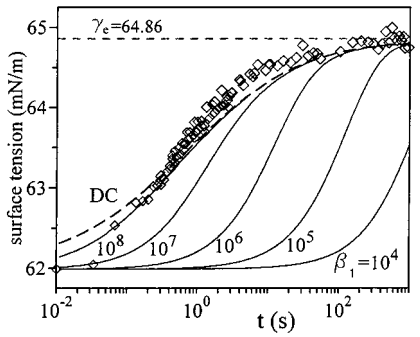

Figure 9. Comparison between $\gamma(t)$ data and the model predictions of mixed-controlled re-equilibration of the GF_2 model for different adsorption rate constants [$\beta_1 = \beta \exp(-E_a^0/RT)$] for 1-nonanol. $C_0 = 7.5 \times 10^{-8}$ mol/cm^3. DC denotes the diffusion-controlled curve.

If the GF_1 model is applied to fit the dynamic $\gamma(t)$ data, the fit is satisfactory (better than F but not as good as GF_2). The diffusivities from GF_1 (the crosses in Figure 8) and GF_2 are pretty close. This is because GF_1, from the best-fit on $\gamma(\Gamma)$, is quite close to GF_2 (Figure 5).

The diffusivity obtained from this work is close to that reported in the literatures for other alcohols. $D = 4.9 \times 10^{-6}$ to 7.3×10^{-6} cm^2/s for 1-octanol, and $D = 5.0 \times 10^{-6}$ to 8.9×10^{-6} cm^2/s for 1-decanol. A comparison of the diffusivities for alcohols from propanol to dodecanol has been detailed in ref 22.

Desorption. The re-equilibration process due to the desorption of 1-nonanol out of a suddenly compressed air−water surface was simulated. Note that the moment at which surface tension was still at equilibrium value (γ_e; at this moment, surface area was A_e and surface concentration was Γ_e) was referenced as the zero time in Figure 6. Data in Figure 6 were re-plotted in Figure 9, and the moment with the lowest surface tension value (γ_b; at this moment, surface area was A_b and surface coverage was Γ_b; point L in Figure 6) was set to be the zero time for the convenience of simulation. A set of surface properties (γ, A, Γ, and the amount of surfactants $A\Gamma$ at surface) during the shrinkage of bubble is listed in Table 2. The data in Table 2 (the column of $A\Gamma$) indicate that the desorption during the ramp-type area change was insignificant for the present system. The number of 1-nonanol molecules desorbed out of the surface during the compression process is therefore neglected in the simulation.

The diffusivity has been obtained from the adsorption experiments ($D = 6.3 \times 10^{-6}$ cm^2/s using the GF_2 model) and is used in the following simulation. If the re-equilibration process was assumed to be diffusion controlled, the diffusion-controlled relaxation profiles by using

Table 2. Relaxations of Surface Properties during the Shrinkage of Bubble

t (s)	γ (mN/m)	A (mm^2)	A_i/A_e	$\Gamma^a \times 10^{10}$ (mol/cm^2)	$A_i\Gamma_i/A_e\Gamma_e$
−1/30	65.13	24.73	1.00	4.179	1.00
0	65.15[b]	24.72	1.00	4.172	1.00
1/30	64.68[c]	24.60	0.99	4.295	1.02
2/30	64.23[c]	21.45	0.87	4.404	0.91
3/30	62.59[c]	20.99	0.85	4.748	0.96
4/30	62.43[c]	20.78	0.84	4.777	0.96
5/30	61.99[d]	20.65	0.84	4.855	0.97
6/30	62.05	20.58	0.83	4.845	0.96
7/30	62.54	20.59	0.83	4.758	0.95

[a] Calculated from surface tension using eq 4 and the generalized Frumkin isotherm. [b] The point right before the desorption process, corresponding to the equilibrium state. [c] The point during the shrinkage of bubble. [d] The point with the lowest surface tension, corresponding to the end of shrinkage and the beginning of the desorption process.

GF_2 model with $D = 6.3 \times 10^{-6}$ cm^2/s are shown in Figure 9. It is clear that the diffusion-limited curve (the dashed curve) describes the $\gamma(t)$ profile of desorption satisfactorily. Therefore, the re-equilibration process is diffusion controlled at $C = 7.5 \times 10^{-7}$ mol/cm^3.

Theoretical Simulation. Many surfactants have been reported as showing transfer-controlled adsorption kinetics.[39−42] For 1-octanol and 1-decanol, the adsorption onto a fresh surface is diffusion controlled.[22] The desorption out of a compressed air−water surface for 1-octanol is diffusion controlled, whereas 1-decanol has a shifting controlling mechanism. In this work, a theoretical simulation was performed for the adsorption of 1-nonanol onto a fresh surface and for the desorption out of a compressed surface. The concentrations considered are 5×10^{-8} to 3.5×10^{-7} mol/cm^3, in which the $\gamma(t)$ profiles are measured in this work. The generalized Frumkin model with $\nu_a = 0$ was picked for the simulation.

Theoretical relaxation profiles, using the GF_2 model, with finite adsorption and desorption rate constants (β and α) are plotted in Figure 9 (the solid curves). The relaxation $\gamma(t)$ profiles depend on bulk concentration (C) and adsorption rate constant β_1 ($= \beta \exp(-E_a^0/RT)$). Simulations of $\gamma(t)$ are performed, in which β_1 varies from diffusion control ($\beta_1 \rightarrow \infty$) to mixed control [$\beta_1 = O(10^5$ or $10^6)$] to sorption kinetic control ($\beta_1 < 10^4$). As discussed in a previous article (Figure 3 in ref 43) and shown in Figure 9, the diffusion-limited curve shows the fastest relaxation; slower relaxations are observed at smaller β_1 because of the increasing kinetic barrier. The distance between the diffusion-limited curve and that for a particular value of β_1 varies gradually with C. The limiting value of β_1 for which the mixed-controlled curve is indistinguishable from diffusion-control profiles is defined as β^l.

The β^l for the adsorption (β^l_{ads}) and desorption (β^l_{des}) processes is plotted in Figure 10 as a function of concentration. The data indicate that, β^l_{ads} is 9×10^7 cm^3/(mol·s) and β^l_{des} for $C = 7.5 \times 10^{-7}$ mol/cm^3 is around 1.2×10^8 cm^3/(mol·s). Since the adsorption process at all 1-nonanol concentrations and the desorption experiment at 7.5×10^{-7} mol/cm^3 are diffusion controlled, it is concluded that $\beta_1 > 1.2 \times 10^8$ cm^3/(mol·s) for 1-nonanol.

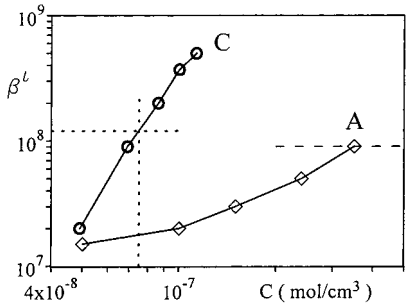

Figure 10. The limiting adsorption rate constant β^l (cm^3 mol^{-1} s^{-1}) as a function of bulk concentration predicted by using the generalized Frumkin model for the adsorption onto a freshly created (A) interface and for the desorption (C) out of a suddenly compressed surface. $D = 6.3 \times 10^{-6}$ cm^2/s and $\nu_a^* = 0$.

Case II. Aggregation Model. In this case, equilibrium $\gamma(C)$ and dynamic $\gamma(t)$ data are applied to determine the model parameters. The process of adsorption onto a freshly created air−water surface is assumed to be diffusion controlled. Dynamic $\gamma(t)$ profiles are also used for the determination of diffusivity.

The parameters that resulted from $\gamma(C)$ and $\gamma(t)$ data are $\Gamma_c = 1.945 \times 10^{-9}$ mol/cm^2, $\omega_1 = 1.89 \times 10^9$ cm^2/mol, $a = 5.18 \times 10^{-6}$ mol/cm^3, and $n = 3.42$. The aggregation model excellently describes $\gamma(C)$ and $\gamma(t)$ data, as shown in Figures 3 and 7. The number of n is a purely fitting value, and the results are consistent with trimer formation. Note that the difference on the dynamic surface tension profiles predicted from the aggregation and GF2 models, as shown in Figure 7, is not too significant but certainly exceeds the error limits of measurement. However, the diffusivity ($D = 1.1 \times 10^{-5}$ cm^2/s) that resulted from the aggregation model and the Ward and Tordai equation (with a planar interface) is larger than that from the generalized Frumkin model with a planar interface ($D = 9.0 \times 10^{-6}$ cm^2/s). $D = 6.3 \times 10^{-6}$ cm^2/s (Figure 8) results when the generalized Frumkin model with a spherical interface (radius = 1 mm) is applied.

6. Conclusions and Discussion

The first approach considers the molecular interaction between the adsorbed molecules. The adsorption of 1-nonanol onto a freshly created air−water interface is found to be cooperative and diffusion controlled, which is the same as 1-octanol and 1-decanol. The desorption out of a suddenly compressed surface is diffusion controlled at $C = 7.5 \times 10^{-7}$ mol/cm^3. A diffusivity of 6.3×10^{-6} cm^2/s results from the best-fit between the dynamic $\gamma(t)$ data and the theoretical profiles predicted from the generalized Frumkin model. A lower limit of adsorption rate constant (1.2×10^8 cm^3/(mol·s) for $\beta \exp(-E_a^0/RT)$), corresponding to a lower limit of desorption rate constant, 4.5×10^2 s^{-1} for $\alpha \exp(-E_d^0/RT)$, is obtained from the simulation.

The second approach assumes that surfactant molecules form two-dimensional aggregates. The aggregation model describes the equilibrium and dynamic surface tension data well with an average aggregation number of $n = 3.42$. This implies that 1-nonanol molecules may aggregate and form clusters within the surface layer.

Data of equation of state, $\gamma(\Gamma/\Gamma_{ref})$, play an important role on determining the model parameters in the first approach. On the aggregation model, both equilibrium $\gamma(C)$ and dynamic $\gamma(t)$ data are needed for determining the model parameters.

There are two major differences between these two approaches or models. First, the (generalized) Frumkin

(39) Li, B.; Geeraerts, G.; Joos, P. *Colloids Surf.* **1994**, *88*, 251.
(40) Chang, H, C.; Hsu, C. T.; Lin, S. Y. *Langmuir* **1998**, *14*, 2476.
(41) Pan, R.; Green, J.; Maldarelli, C *J. Colloid Interface Sci.* **1998**, *205*, 213.
(42) Lin, S. Y.; Tsay, R. Y.; Lin, L. W.; Chen, S. I. *Langmuir* **1996**, *12*, 6530.
(43) Lin, S. Y.; Chang, H. C.; Chen, E. M. *J. Chem. Eng. Jpn.* **1996**, *29*, 634.

model assumes a homogeneous surfactant monolayer at fluid−liquid interface and the molecular interaction between the adsorbed surfactant molecules is significant. A linear or power law dependence on the surface concentration is taken into account to simulate the effect of molecular interaction. On the other hand, the aggregation model assumes that surfactant molecules aggregate and form a second liquid-expanded phase. The surface is therefore occupied by both surfactant monomers and aggregates. The second difference is that the aggregation model works only for surfactant molecules with cooperative forces. The Frumkin-type model can work for both cooperative and anti-cooperative surfactants. More interpretation on the nature of the condensed phase has been discussed by Lin et al. in ref 1.

Acknowledgment. This work was supported by the National Science Council of Taiwan, Republic of China (Grant NSC 89-2214-E-011-021).

LA011418T